

# Ground states of helium to neon and their ions in strong magnetic fields

Sebastian Boblest, Christoph Schimeczek, and Günter Wunner

*Institut für Theoretische Physik 1, Universität Stuttgart, D-70550 Stuttgart, Germany*

(Received 29 October 2013; published 10 January 2014)

We use the combination of a two-dimensional Hartree-Fock and a diffusion quantum Monte Carlo method, both of which we recently presented in this journal [C. Schimeczek *et al.*, *Phys. Rev. A* **88**, 012509 (2013)], for a thorough investigation of the ground state configurations of all atoms and ions with  $Z = 2-10$  with the exception of hydrogen-like systems in strong magnetic fields. We obtain the most comprehensive data set of ground state configurations as a function of the magnetic field strength currently available and hence are able to analyze and compare the properties of systems with different core charges and electron numbers in detail.

DOI: [10.1103/PhysRevA.89.012505](https://doi.org/10.1103/PhysRevA.89.012505)

PACS number(s): 31.15.xr, 31.15.ve, 31.15.ag, 32.60.+i

## I. INTRODUCTION

In the last years many research groups have added to the understanding of atomic and molecular systems in strong magnetic fields applying different Hartree-Fock methods [1–7], density functional theory [8], and configuration interaction calculations [9–15]. Recently, we presented a new combination of a two-dimensional Hartree Fock method (2DHFR) with a fixed phase diffusion quantum Monte Carlo code (FPDQMC) for the computation of energy levels of atoms in intermediately strong to very strong magnetic fields [16]. These methods are capable of computing very accurate energy values of atomic states for all field strengths  $\beta_Z \gtrsim 0.1$ , where  $\beta_Z = \beta/Z^2 = B/(B_0 Z^2)$ , with  $B_0 \approx 4.70103 \times 10^5$  T, is the nuclear-charge-scaled magnetic field strength. We apply this combination of the two methods to reveal the electronic ground state configurations of all elements from helium to neon and their positive ions with two or more electrons for such magnetic field strengths.

In very strong magnetic fields ( $B \gtrsim 10^7$  T) the spin-flip energies are much larger than the atomic single-particle energies, and therefore in bound states all electron spins are aligned antiparallel to the field. This is no longer true when the magnetic field decreases and the spin-flip energies come into the range of the single-particle energies. Then, a transition from a fully spin-polarized state to a state with mixed alignments of the electron spins occurs. The ground state energies and configurations of atoms and ions in strong magnetic fields are of special interest for astrophysical applications. Ground state and excitation energies are the basis to find Boltzmann weights and to calculate partition functions and ionization fractions (see, e.g., [17,18]). Thus they are of utter importance for the modeling of neutron star atmospheres (see, e.g., [19,20]), a discipline always hampered by the lack of atomic data for strong fields.

In this direction, Ivanov and Schmelcher [1–3] conducted several studies with a two-dimensional Hartree-Fock mesh approach. Reference [1] is devoted to the study of the ground state configurations of Li and Li<sup>+</sup> and covers all magnetic field strengths from  $B = 0$  T up to the high-field regime. This study revealed three ground state configurations for Li and two for Li<sup>+</sup>. The ground state configuration of neutral carbon was investigated in Ref. [2], again from  $B = 0$  T up to the high-field regime. In this case, seven different ground state configurations were found. In Ref. [3] the authors went in a slightly different direction. There, they focused on the high-field regime and

studied the transition from the high-field ground state to other configurations for all atoms and singly positive ions from helium to neon. To our knowledge, there is no further systematic investigation of the ground state configurations of atoms in strong magnetic fields available in the literature.

We therefore take over from where this last investigation stopped and study all atoms and ions from helium to neon with at least two electrons. The study of hydrogen-like systems is superfluous in this context, as their ground state configuration is independent of the magnetic field strength. For the hydrogen atom a large amount of accurate data [21–23] over a wide range of  $\beta$  is available and it is well known that the energies and wave functions of hydrogen-like systems are related to those of the hydrogen atom by simple scaling laws [9,21,24].

The many-particle Hamiltonian in cylindrical coordinates reads

$$\hat{H} = \sum_{i=1}^{N_e} \left( -\frac{1}{2} \Delta_i - i\beta \partial_{\varphi_i} + \frac{1}{2} \beta^2 \rho_i^2 + 2\beta m_{s_i} - \frac{Z}{|\mathbf{r}_i|} + \sum_{j=i+1}^{N_e} \frac{1}{|\mathbf{r}_i - \mathbf{r}_j|} \right) \quad (1)$$

and describes  $N_e$  electrons with spin  $m_{s_i}$  in the potential of a nucleus with charge  $Z$  and infinite mass. We use atomic hartree units throughout this paper. We do not consider relativistic corrections, as they are expected to be small, even at large magnetic field strengths [25,26]. Also, we assume a vanishing pseudomomentum for the center of mass (see Schmelcher and Cederbaum [27]). This assumption fails for charged systems  $N \neq Z$  as the internal and external motion of ions is coupled and their description is in general much more complicated (see, e.g., [28–30]). A complete theoretical description of this problem is still lacking; thus we note that the accuracy of our results might be limited for charged systems.

In the following we give a short summary of our solution method. A detailed description can be found in our previous paper [16]. In the 2DHFR method the many-particle wave function is constructed from a Slater determinant of single-particle spin orbitals  $\psi^i$  for each electron  $i$ . These are expanded using a full 2D description in terms of Landau channels:

$$\psi^i(\rho_i, \varphi_i, z_i) = \sum_{n=0}^{N_L} P_n^i(z_i) \Phi_{nm_i}(\rho_i, \varphi_i), \quad (2)$$

where each channel contributes with an individual longitudinal wave function  $P_n^i(z_i)$ , which is expanded with  $B$  splines [31]  $B_\mu$  on a finite element grid:

$$P_n^i(z_i) = \sum_\nu \alpha_{n\nu}^i B_\nu^i(z_i). \quad (3)$$

The variation of the energy functional with respect to the  $B$ -spline coefficients  $\alpha_{n\mu}$  yields two-dimensional Hartree-Fock-Roothaan equations, which are solved iteratively. The initial wave functions are given by the approximate solutions found by our HFFER II code, described in [32]. We include up to  $N_L = 30$  Landau channels for the single-particle Landau expansion and thereby obtain accurate results down to  $\beta_Z \approx 0.1$ .

Subsequent to the 2DHFR calculations we improve our energy-estimates in a FPDQMC procedure [33], where we simulate the importance sampled imaginary-time ( $\tau = it$ ) Schrödinger equation. With the single-electron orbitals from 2DHFR, we construct a trial function  $\Psi_T$  of the usual form [34]:

$$\Psi_T(\mathbf{R}) = \mathcal{J} \Psi_\downarrow(\mathbf{R}) \Psi_\uparrow(\mathbf{R}). \quad (4)$$

Here,  $\Psi_\downarrow$  and  $\Psi_\uparrow$  are Slater determinants of all spin-down and spin-up electrons, respectively, and  $\mathcal{J}$  is a Padé-Jastrow factor [34], whose free parameters are optimized in a variational quantum Monte Carlo simulation using correlated sampling.

The trial function is used to guide an ensemble of random walkers through configuration space. The FPDQMC method redistributes this ensemble, initially distributed according to  $|\Psi_T|^2$ , such that it represents  $|\Psi_T \phi_0|$ , where  $\phi_0$  is the ground state of the symmetry subspace of  $\Psi_T$ ; i.e., excited state contributions are damped as the imaginary time progresses.

When the ensemble has been redistributed, we obtain an energy estimate by evaluating the local energy  $E_L(\mathbf{R}) = \hat{H} \Psi_T(\mathbf{R}) / \Psi_T(\mathbf{R})$  at all walker positions in a given number of steps. The FPDQMC method has the limitation of keeping the phase of the trial function fixed during the simulation; thus the results contain a fixed-phase error. However, the method is variational and the phase error is very small. For helium, we found a maximum error of only 2‰ in the most extreme cases [16].

## II. PRELIMINARY REMARKS

The exploration of ground state configurations of atoms and ions over a wide range of magnetic field strengths is the natural next step after computing ground state energies for several explicit magnetic field strengths as we did in Ref. [16]. To do so, extensive numerical calculations are required after identifying possible candidates for the ground state configurations by qualitative arguments; see also the extensive discussion in Ref. [3]. Our combination of the very fast 2DHFR method and the very accurate FPDQMC method is ideally suited for such a task. With 2DHFR, we analyze the energies of possible ground state configurations by performing many calculations over wide ranges of magnetic field strengths  $\beta$ . In this way, we obtain first estimates for the magnetic field strengths, where the ground state configuration changes. Then, we conduct more accurate FPDQMC calculations for  $\beta$  values close to the crossing points predicted with 2DHFR to obtain our final results. As we already have a very good idea of where the configurations cross after our 2DHFR calculations, we can

choose a very fine grid in  $\beta$  for our FPDQMC calculations, and therefore find very accurate values for the crossing points.

### A. Ground state regimes

In the presence of a magnetic field an atom and its physics are subject to a variety of changes. First, the conserved quantum numbers are reduced to the total angular momentum  $z$  projection  $M$ , the total  $z$  parity  $\Pi_z$ , the total spin  $z$  projection  $S_z$ , and the total spin  $S^2$ . In contrast to full configuration interaction methods based on Slater determinants (see Knowles and Handy [35]) our wave functions are spin contaminated if different spin orientations are involved, a consequence of the two Slater determinants in the FPDQMC approach given in Eq. (4). However, this does not affect our precision during the search for the ground states. The remaining quantum numbers define a subspace and states are labeled by their excitation level  $\nu$  within this subspace:  $\{-M, \Pi_z, S_z, \nu\}$ . Since the wave functions and energies of the states strongly depend on the magnetic field strength, the ground state energy and configuration are also affected by the magnetic field. In hydrogen-like systems the ground state is always the lowest state of the  $\{0, +, \downarrow\}$  subspace. In multielectron systems, however, the ground state configuration varies in dependence of the magnetic field strength. Due to the noncrossing theorem of states corresponding to the same symmetry subspace [36], ground state configuration changes correspond to the crossing of the lowest states of different symmetry subspaces.

Within the Hartree-Fock approximation we assign single-particle quantum numbers  $(-m_i, \pi_{z_i}, m_{s_i}, \bar{\nu}_i)$  to each orbital. Both sets of quantum numbers are connected by the relations

$$M = \sum_{i=1}^{N_e} m_i, \quad S_z = \sum_{i=1}^{N_e} m_{s_i}, \quad \Pi = \sum_{i=1}^{N_e} \pi_{z_i}. \quad (5)$$

The energy of orbitals with positive  $m$  or  $m_s$  is raised by  $2\beta m$  or  $2\beta$  in atomic units in comparison to their counterparts with negative  $m$  or  $m_s$ , respectively. These orbitals are therefore no candidates for the ground states at larger  $\beta_Z$ . One can define four regimes for the ground state configurations: the low-field regime (LF), the magnetic polarization regime (MP) with partial spin polarization (PSP), the regime of full spin polarization (FSP), and the high-field ground state regime (HFGS). In the MP regime the ground state configuration contains only orbitals with  $m \leq 0$ . To estimate the transition field strength to this regime we examine the single-particle orbital  $(-1, +, \downarrow, 1)$ , which corresponds to the field free state  $2p_{+1}$  and has the lowest energy of all orbitals with positive  $m$ . In neutral carbon this orbital is no longer contained in the ground state configuration at  $\beta_Z \approx 7 \times 10^{-3}$  [2]; thus we can safely ignore these states in this investigation. The ground state reaches full spin polarization roughly at  $\beta_Z \approx 0.1$ . Then, all spins are aligned antiparallely to the magnetic field. Eventually, the high-field ground state configuration is reached at large  $\beta_Z$ . There, all electrons occupy tightly bound orbitals ( $\bar{\nu} = 1, \pi_z = 1$ ), the lowest lying orbital with positive  $z$  parity of each  $m$ .

Due to our Landau ansatz for the single-particle wave functions [16,21] we are restricted to  $\beta_Z \gtrsim 0.1$  and list transitions only for these field strengths. Thus, we cannot investigate ground state configurations in the LF regime or

the transition to the MP regime. To facilitate the comparison with the literature, we adopt the orbital labeling introduced by Ivanov [3], which is useful at high  $\beta_Z$ : We assume a HFGS configuration and denote only those orbitals that deviate from this configuration by their zero-field quantum numbers  $nl_m^{(\uparrow)}$  (see also [37]). Also, we only indicate the spin alignment ( $\uparrow$ ) if it deviates from the FSP. This allows for a very compact representation of the orbital configuration, even for many electrons, at high  $\beta_Z$ . The high-field ground state is then denoted by 0. The relevant fully spin-polarized states for this work are 0,  $2p_0$ , and  $2p_03d_{-1}$ .

### B. Computation of transition field strengths

We determine a precise estimate for the transition point ( $\beta_Z^{\text{Tr}}$ ,  $E^{\text{Tr}}$ ) between two states  $A$  and  $B$  by a linear interpolation of the energy functions  $E(\beta_Z)$  from four  $E(\beta)$  values in the vicinity of the transition point. As we choose very small intervals  $\Delta\beta_Z$ , which are adapted to each of the crossing points, this linear interpolation causes only insignificant deviations compared to an interpolation of higher order. We account for the statistical uncertainties of our FPDQMC results by error propagation, yielding statistical  $1\sigma$  uncertainties also for the crossing field strengths and energies. Values in brackets thereby denote this statistical uncertainties of the last digit(s).

In general, due to the rather low field strengths, we obtain corrections of energy values in FPDQMC with respect to the 2DHFR results of around 2% for PSP states and  $\lesssim 1\%$  for FSP states. This is caused by the large spherical-symmetric component of the innermost orbital, resulting in difficult convergence of the employed single-particle Landau expansion. The different corrections for PSP and FSP states lead to slightly larger values of  $\beta_Z$  for the change of regime that we find in FPDQMC calculations compared to the corresponding 2DHFR values. This is symbolically depicted in Fig. 1. The 2DHFR predictions for transition field strengths deviate from the precise FPDQMC results by up to 4%. Thus, all numerical values are taken from our FPDQMC calculations in what follows.

## III. RESULTS AND DISCUSSION

### A. 2–4 electron systems

We start our discussion with systems of 2–4 electrons. Here, only the 0 and  $1s^\uparrow$  configurations are possible ground

TABLE I. Magnetic field strengths  $\beta_Z^{\text{Tr}}$  and energy values  $E^{\text{Tr}}$  in hartrees at the  $1s^\uparrow$ -0 ground state configuration change for helium-like, lithium-like, and beryllium-like ions.

Z	Helium-like		Lithium-like		Beryllium-like	
	$\beta_Z^{\text{Tr}}$	$E^{\text{Tr}}[-\text{Ha}]$	$\beta_Z^{\text{Tr}}$	$E^{\text{Tr}}[-\text{Ha}]$	$\beta_Z^{\text{Tr}}$	$E^{\text{Tr}}[-\text{Ha}]$
2	0.09393(4)	2.8010(2)				
3	0.11744(3)	6.9766(3)	0.12212(3)	7.6905(3)		
4	0.12993(4)	13.0453(6)	0.14229(4)	15.0670(6)	0.14432(4)	15.9779(7)
5	0.13763(4)	21.0082(8)	0.15510(4)	24.9386(9)	0.16023(4)	27.1632(10)
6	0.14292(4)	30.8640(13)	0.16404(4)	37.309(2)	0.17145(4)	41.356(2)
7	0.14675(3)	42.618(2)	0.17059(3)	52.184(2)	0.17979(3)	58.562(2)
8	0.14960(3)	56.260(2)	0.17556(3)	69.551(2)	0.18627(3)	78.775(3)
9	0.15189(3)	71.805(3)	0.17947(4)	89.418(4)	0.19137(3)	102.000(3)
10	0.15372(3)	89.235(4)	0.18266(3)	111.783(4)	0.19547(3)	128.218(4)

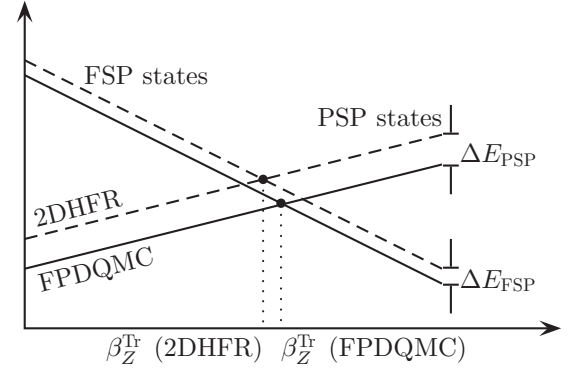


FIG. 1. The larger energy corrections in FPDQMC (solid lines) with respect to 2DHFR (dashed lines) for PSP states compared to those for FSP states cause slightly larger predicted values  $\beta_Z^{\text{Tr}}$  for the transitions between such states in FPDQMC compared to the values in 2DHFR.

states for  $\beta_Z \gtrsim 0.1$ . The  $1s^\uparrow$  configuration is the zero-field configuration for 2-electron systems. Table I shows the results for the transition field strengths  $\beta_Z^{\text{Tr}}$ . In addition we also give the corresponding energies  $E^{\text{Tr}}$  for these transitions to allow for a comparison in future studies. We see that the nuclear charge scaled magnetic field strength  $\beta_Z$  of this transition slowly increases with  $Z$ . It is reasonable to assume that the transition field strength for two-electron systems in the limit of  $Z \rightarrow \infty$  asymptotically approaches the value  $\beta_\infty^{\text{Tr}} = 0.17058$ . At this  $\beta$  the energy curves of the hydrogen orbitals  $1s^\uparrow$  and  $2p_{-1}$  intersect [21–23]. With increasing nuclear charge the electron-electron interaction terms become less important compared to the nuclear potential and can be neglected in this limit. We have visualized this behavior with additional calculations for  $Z = 11$ – $26$  and  $Z = 92$  in Fig. 2. In the last case we found  $\beta_Z^{\text{Tr}} = 0.16882(3)$ , which deviates by only 1% from the asymptotic value. This increase of  $\beta_Z^{\text{Tr}}$  with  $Z$  is a shared feature of all ground state transitions we studied.

### B. Systems with 5 and more electrons

We found four different ground state configurations for the 5-electron systems, as is shown in Table II. At the lowest investigated field strengths  $\beta_Z \approx 0.1$  the configuration  $1s^\uparrow 2p_0$

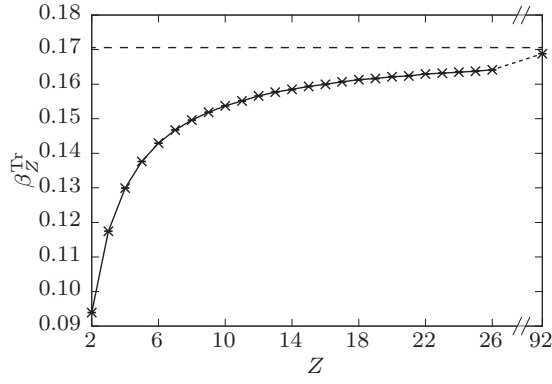


FIG. 2. Magnetic field strength  $\beta_Z^{\text{Tr}}$  of the  $1s^\uparrow-0$  ground state configuration change for helium-like ions with  $Z = 2-26$  and  $92$ . The dashed line denotes the field strength  $\beta_\infty^{\text{Tr}} = 0.17058$ , where the energies of the hydrogen states  $1s^\uparrow$  and  $2p_{-1}$  coincide.

forms the ground state for all investigated boron-like ions but not for neutral boron. Also, the  $1s^\uparrow$  and  $2p_0$  configurations represent ground states at intermediate field strengths. For neutral boron our results differ from those in Ref. [3], where the direct transition  $1s^\uparrow-0$  was found. Figure 3 shows the progression of the energy functions  $E(\beta_Z)$  of the two configurations  $2p_0$  and  $0$  of this system. Since the two energy functions intersect at a very small angle, small differences in the computed energy values for these two configurations lead to large differences for the proposed transition field strengths, the cause for the differing predictions in Ref. [3].

For  $\text{C}^+$  the configuration  $1s^\uparrow 2p_0$  becomes ground state at field strengths  $\beta_Z < 0.0788(7)$ . In this case, we push our 2DHFR ansatz down towards a critically low magnetic field. However, we found that our FPDQMC results are still very accurate even for such small magnetic fields. Still, we cannot calculate reliably the transition field strength to  $1s^\uparrow 2p_0$  for neutral boron, which occurs at even lower field strengths.

The 6-electron systems are especially interesting. Here, we find two possible paths from the configuration  $1s^\uparrow 2p_0$  at the lowest available field strengths to the high-field configuration (Table III). For  $Z = 6$  and  $Z = 7$  we found the path  $1s^\uparrow 2p_0-1s^\uparrow 2p_0-0$ , whereas for  $Z = 8-9$ , the configuration  $1s^\uparrow$  is never ground state and we find the transitions  $1s^\uparrow 2p_0-2p_0-0$  instead. This indicates that for  $\text{N}^+$  and  $\text{O}^{2+}$  the configurations  $1s^\uparrow$  and  $1s^\uparrow 2p_0$  should have almost the same energies in the relevant region of  $\beta_Z$ . Indeed, for  $\text{O}^{2+}$  the transitions  $1s^\uparrow 2p_0-$

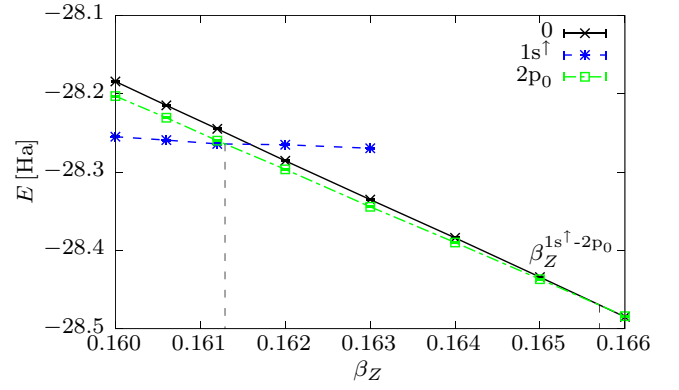


FIG. 3. (Color online) Energies of the  $2p_0$ ,  $1s^\uparrow$ , and  $0$  ground state candidates for neutral boron in the neighborhood of their crossing points. Lines serve as a guide to the eye.

$1s^\uparrow$  at  $\beta_Z^{\text{Tr}} = 0.1855(7)$  and  $1s^\uparrow 2p_0-2p_0$  at  $\beta_Z^{\text{Tr}} = 0.18445(3)$  occur at very similar field strengths; see Fig. 4. The energy functions of  $1s^\uparrow 2p_0$  and  $1s^\uparrow$  progress almost in parallel, which causes a higher uncertainty in the transition field strength between these two states compared to the one for the transition  $1s^\uparrow 2p_0-2p_0$ . Still, our results are accurate enough to exclude  $1s^\uparrow$  as ground state configuration.

The nitrogen-like, oxygen-like, and fluorine-like systems show, similarly to the 6-electron systems with  $Z = 8-10$ , only the ground state transitions  $1s^\uparrow 2p_0-2p_0$  and  $2p_0-0$ , as is presented in Table IV.

In neutral neon, however, we find for the first time the ground state configuration  $2p_0 3d_{-1}$ ; see Table V. Here, our results again differ qualitatively from those in Ref. [3], where  $2p_0 3d_{-1}$  was excluded as ground state configuration. However, the authors of Ref. [3] themselves stated that in more accurate studies  $2p_0 3d_{-1}$  might be revealed to be ground state in neutral neon in a short interval of magnetic field strengths. Indeed, the transition  $1s^\uparrow 2p_0-2p_0 3d_{-1}$  occurs at  $\beta_Z = 0.20346(3)$  and the transition  $2p_0 3d_{-1}-2p_0$  already at  $\beta_Z = 0.2089(6)$ . The configuration  $2p_0$  then is the ground state up until  $\beta_Z = 0.8076(4)$ , before the change to the high-field configuration occurs.

### C. Transitions to the FSP and HFGS regimes

The regime of fully spin polarized ground states and the high-field ground state are of special interest. The latter is important as in this regime the ground state configuration

TABLE II. Transitions of ground state configurations for boron-like ions. The  $1s^\uparrow 2p_0-1s^\uparrow$  transition in neutral boron is not accessible in our approach.

Z	$1s^\uparrow 2p_0-1s^\uparrow$		$1s^\uparrow-2p_0$		$2p_0-0$	
	$\beta_Z^{\text{Tr}}$	$E^{\text{Tr}}[-\text{Ha}]$	$\beta_Z^{\text{Tr}}$	$E^{\text{Tr}}[-\text{Ha}]$	$\beta_Z^{\text{Tr}}$	$E^{\text{Tr}}[-\text{Ha}]$
5			0.16129(4)	28.2640(10)	0.1657(3)	28.47(2)
6	0.0788(7)	41.67(3)	0.17206(4)	43.799(2)	0.2067(3)	46.13(2)
7	0.1013(6)	60.33(3)	0.17993(4)	62.768(3)	0.2378(3)	68.06(3)
8	0.1191(5)	82.47(3)	0.18600(4)	85.178(4)	0.2622(3)	94.27(3)
9	0.1332(4)	108.08(3)	0.19083(3)	111.029(4)	0.2816(3)	124.73(4)
10	0.1450(4)	137.17(3)	0.19472(4)	140.317(5)	0.2971(3)	159.39(5)



TABLE III. Transitions of ground state configurations for carbon-like ions.

Z	$1s^\uparrow 2p_0 - 1s^\uparrow$		$1s^\uparrow - 2p_0$		$1s^\uparrow 2p_0 - 2p_0$		$2p_0 - 0$	
	$\beta_Z^{\text{Tr}}$	$E^{\text{Tr}}[-\text{Ha}]$	$\beta_Z^{\text{Tr}}$	$E^{\text{Tr}}[-\text{Ha}]$	$\beta_Z^{\text{Tr}}$	$E^{\text{Tr}}[-\text{Ha}]$	$\beta_Z^{\text{Tr}}$	$E^{\text{Tr}}[-\text{Ha}]$
6	0.1170(7)	43.91(2)	0.17000(3)	45.023(2)			0.2693(4)	51.61(2)
7	0.1538(7)	64.65(2)	0.17805(4)	65.342(3)			0.3181(3)	78.03(3)
8					0.18445(3)	89.501(3)	0.3571(3)	109.94(3)
9					0.19085(3)	117.737(4)	0.3880(3)	147.33(4)
10					0.19615(3)	149.891(5)	0.4141(4)	190.27(6)

is independent of  $\beta$ , whereas in the former regime one can disregard orbitals with spin-up alignment for ground state configurations. Both facts correspond to a significant reduction in numbers of lowly excited electronic configurations. Therefore we expect considerable effects on the partition functions and thus the ionization balances of atoms and ions in different regimes of the magnetic field strength.

For the 2–4 electron systems, these regime changes coincide and correspond to the ground state transition  $1s^\uparrow - 0$ . All other investigated systems have one additional FSP configuration besides the HFGS, namely  $2p_0$ , with the exception of neutral neon with two additional configurations  $2p_0$  and  $2p_0 3d_{-1}$ . In Table VI we sum up the magnetic field strengths for PSP-FSP transitions for all systems studied in this paper. We see that not only these transition field strengths increase monotonically with increasing  $Z$  at constant  $N_e$ , which we have explained before, but also with increasing  $N_e$  while  $Z$  is kept fixed. We suggest the following explanation for the latter finding: The orbitals  $2p_0$  or  $3d_{-1}$  are considerably stronger affected by the electronic repulsion that increases with  $N_e$  in comparison to the inner orbital  $1s^\uparrow$ , whose shape and energy is mostly unaffected by a larger number of electrons. Thus, the PSP ground state prevails up to higher values of  $\beta_Z$  for larger electron numbers. The only exceptions to this rule were found for boron-like and carbon-like systems, where  $\beta_Z$  of the PSP-FSP transition drops coming from  $N_e = 4$  but then rises again at  $N_e = 7$ . This is caused by different ground state configurations involved at this change of regimes. Up to 4 electrons this change corresponds to the transition  $1s^\uparrow - 0$ , but for higher  $N_e$  other transitions are involved.

The magnetic field strength corresponding to the onset of the HFGS regime is commonly estimated with the condition  $\beta_Z \gg Z$  [19]. Our calculations show that this estimate yields too large a  $\beta_Z$  for small values of  $Z$  and  $N_e$ ; see Table VII. However, we indeed see that the field strength  $\beta_Z$  that marks the verge of the HFGS strongly increases with  $Z$  and  $N_e$ , i.e., from  $\beta_Z = 0.09393(4)$  for neutral helium to  $\beta_Z = 0.8076(4)$  for neutral neon.

#### D. Comparison with the literature

We end the discussion of our results with a comparison with the findings of Ivanov and Schmelcher [2,3]. Their method, as well as our FPDQMC, are variational, so we are sure that higher binding energies correspond to more accurate results. A direct comparison is complicated by the fact that we and Ivanov and Schmelcher did not compute binding energies for exactly the same  $\beta_Z$ . Hence, we linearly interpolate our results to be able to compare with the energy values given in Ref. [3]. The results of this comparison are shown in Table VIII. We focus on the transitions at low  $\beta_Z$  as our employed Landau ansatz is especially prone to errors in this magnetic field strength regime. In all cases our binding energies are slightly higher than those given in Ref. [3], for both states in question. In addition, our calculations feature a higher data point density. Therefore, we can assume that our transition field strengths are also more accurate.

In Table IX we compare the transition field strengths for various ground state configuration changes with those of

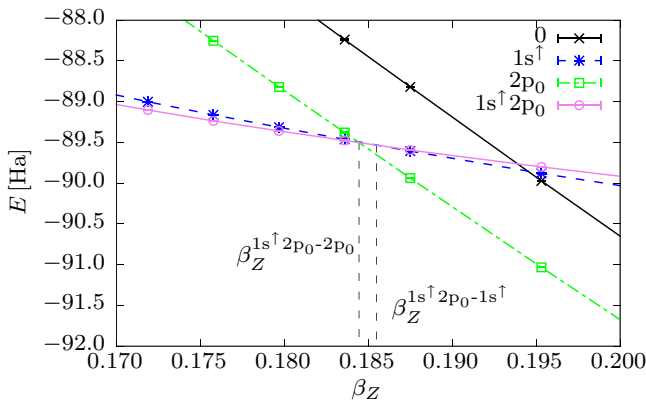


FIG. 4. (Color online) Energies of  $O^{2+}$  ground state candidates at the edge of the FSP regime. Lines serve as a guide to the eye.

TABLE IV. Transitions of ground state configurations for nitrogen-like ions, oxygen-like ions, and fluorine-like ions.

Z	$1s^\uparrow 2p_0 - 2p_0$		$2p_0 - 0$	
	$\beta_Z^{\text{Tr}}$	$E^{\text{Tr}}[-\text{Ha}]$	$\beta_Z^{\text{Tr}}$	$E^{\text{Tr}}[-\text{Ha}]$
Nitrogen-like				
7	0.17812(4)	66.838(3)	0.3864(4)	85.31(3)
8	0.18678(4)	92.768(4)	0.4430(3)	122.52(3)
9	0.19388(3)	123.029(5)	0.4894(3)	166.54(4)
10	0.19978(3)	157.618(5)	0.5279(3)	217.35(4)
Oxygen-like				
8	0.18781(3)	94.545(4)	0.5172(4)	131.90(4)
9	0.19550(3)	126.460(4)	0.5805(3)	181.94(4)
10	0.20191(3)	163.091(6)	0.6335(4)	240.11(5)
Fluorine-like				
9	0.19649(4)	128.367(5)	0.6581(6)	193.41(7)
10	0.20311(3)	166.688(6)	0.7071(4)	258.27(5)

TABLE V. Transitions of ground state configurations in neutral neon.

Z	$1s^{\uparrow}2p_0-2p_03d_{-1}$		$2p_03d_{-1}-2p_0$		$2p_0-0$	
	$\beta_Z^{\text{Tr}}$	$E^{\text{Tr}}[-\text{Ha}]$	$\beta_Z^{\text{Tr}}$	$E^{\text{Tr}}[-\text{Ha}]$	$\beta_Z^{\text{Tr}}$	$E^{\text{Tr}}[-\text{Ha}]$
10	0.20346(3)	168.685(6)	0.2089(6)	170.07(14)	0.8076(4)	272.04(6)

TABLE VI. Magnetic field strength  $\beta_Z^{\text{Tr}}$  at the transition from PSP to FSP for all systems.

Z	$N_e = 2$	$N_e = 3$	$N_e = 4$	$N_e = 5$	$N_e = 6$	$N_e = 7$	$N_e = 8$	$N_e = 9$	$N_e = 10$
2	0.09393(4)								
3	0.11744(3)	0.12212(3)							
4	0.12993(4)	0.14229(4)	0.14432(4)						
5	0.13763(4)	0.15510(4)	0.16023(4)	0.16129(4)					
6	0.14292(4)	0.16404(4)	0.17145(4)	0.17206(4)	0.17000(3)				
7	0.14675(3)	0.17059(3)	0.17979(3)	0.17993(4)	0.17805(4)	0.17812(4)			
8	0.14960(3)	0.17556(3)	0.18627(3)	0.18600(4)	0.18445(3)	0.18678(4)	0.18781(3)		
9	0.15189(3)	0.17947(4)	0.19137(3)	0.19083(3)	0.19085(3)	0.19388(3)	0.19550(3)	0.19649(4)	
10	0.15372(3)	0.18266(3)	0.19547(3)	0.19472(4)	0.19615(3)	0.19978(3)	0.20191(3)	0.20311(3)	0.20346(3)

TABLE VII. Magnetic field strength  $\beta_Z^{\text{Tr}}$  at the transition to the HFGS configuration for all systems.

Z	$N_e = 2$	$N_e = 3$	$N_e = 4$	$N_e = 5$	$N_e = 6$	$N_e = 7$	$N_e = 8$	$N_e = 9$	$N_e = 10$
2	0.09393(4)								
3	0.11744(3)	0.12212(3)							
4	0.12993(4)	0.14229(4)	0.14432(4)						
5	0.13763(4)	0.15510(4)	0.16023(4)	0.1657(3)					
6	0.14292(4)	0.16404(4)	0.17145(4)	0.2067(3)	0.2693(4)				
7	0.14675(3)	0.17059(3)	0.17979(3)	0.2378(3)	0.3181(3)	0.3864(4)			
8	0.14960(3)	0.17556(3)	0.18627(3)	0.2622(3)	0.3571(3)	0.4430(3)	0.5172(4)		
9	0.15189(3)	0.17947(4)	0.19137(3)	0.2816(3)	0.3880(3)	0.4894(3)	0.5805(3)	0.6581(6)	
10	0.15372(3)	0.18266(3)	0.19547(3)	0.2971(3)	0.4141(4)	0.5279(3)	0.6335(4)	0.7071(4)	0.8076(4)

TABLE VIII. Binding energies in atomic hartree units of ground state candidates at the transition field strength predicted in Ref. [3] as well as their corresponding energy result. Our first and second listed energies  $E_1$  and  $E_2$  correspond to the first and second listed state in the transition, respectively.

Z	Transition	$\beta_Z^{\text{Tr}}$	$E_1$	$E_2$	Ref. [3]
2	$1s^{\uparrow}-0$	0.0889	2.81133(19)	2.77385(14)	2.76940
3	$1s^{\uparrow}-0$	0.1196	7.69456(31)	7.65409(17)	7.64785
4	$1s^{\uparrow}-0$	0.1427	15.9780(7)	15.9310(4)	15.91660
5	$1s^{\uparrow}-0$	0.1605	28.2584(10)	28.2098(6)	28.18667
6	$1s^{\uparrow}-2p_0$	0.1697	45.0183(12)	44.9974(8)	44.93410
7	$1s^{\uparrow}2p_0-2p_0$	0.1775	66.8237(17)	66.7729(11)	66.69306
8	$1s^{\uparrow}2p_0-2p_0$	0.1874	94.5279(22)	94.4792(13)	94.37730
9	$1s^{\uparrow}2p_0-2p_0$	0.1959	128.3431(28)	128.2893(16)	128.16050
10	$1s^{\uparrow}2p_0-2p_0$	0.2034	168.6763(32)	168.6265(18)	168.47340

TABLE IX. Comparison of magnetic field strengths  $\beta_Z^{\text{Tr}}$  at ground state transitions with results in Ref. [3] for neutral atoms and singly positive ions. Values marked with \* represent transitions that are only ground state transitions in the corresponding work. The transition  $2p_03d_{-1}-2p_0$  in neutral neon and the transition  $1s^{\uparrow}2p_0-1s^{\uparrow}$  in neutral carbon discussed in Ref. [2] are given in the text.

Z	$1s^{\uparrow}-0$		$1s^{\uparrow}-2p_0$		$1s^{\uparrow}2p_0-2p_0$		$2p_0-0$	
	FPDQMC	Ref. [3]	FPDQMC	Ref. [3]	FPDQMC	Ref. [3]	FPDQMC	Ref. [3]
Neutral atoms								
2	0.09393(4)	0.0889						
3	0.12212(3)	0.1196						
4	0.14432(4)	0.1427						
5		0.1605*	0.16129(4)*	0.16065			0.1657(3)*	0.1585
6			0.17000(3)	0.16967			0.2693(4)	0.25922
7					0.17812(4)	0.17753	0.3864(4)	0.37601
8					0.18781(3)	0.18738	0.5172(4)	0.50563
9					0.19550(3)	0.19590	0.6581(6)	0.645988
10					0.20364(3)	0.20336*	0.8076(4)	0.795690
Singly positive ions								
3	0.11744(3)	0.11510						
4	0.14229(4)	0.1407						
5	0.16023(4)	0.1591						
6			0.17206(4)	0.17154			0.2067(3)	0.20189
7			0.17805(4)	0.17785			0.3181(3)	0.31132
8					0.18678(4)	0.18632	0.4430(3)	0.43552
9					0.19550(3)	0.19514	0.5805(3)	0.57175
10					0.19649(4)	0.20280	0.7071(4)	0.718020

Ref. [3]. In order to keep the table compact, we omitted the transitions  $1s_0^{\uparrow}2p_0-1s_0^{\uparrow}$ , occurring only in neutral carbon, and  $2p_03d_{-1}-2p_0$ , relevant only in neutral neon. For the first one, Ivanov and Schmelcher [2] found  $\beta_Z = 0.1100$  compared to  $\beta_Z = 0.1170(7)$  in our study. The second transition is only identified as a ground state configuration change by us at  $\beta_Z = 0.2089(6)$ , whereas the study [3] found  $\beta_Z = 0.20269$ . Altogether, the results are in good agreement, showing maximum deviations around 3%. Thus, besides the two cases where Ivanov and Schmelcher predicted a different ground state sequence due to a very small crossing angle of the energy curves, we confirm the findings of that study.

#### IV. CONCLUSION AND OUTLOOK

In this paper, we analyzed the electronic configuration of the ground states of all systems with  $Z = 2-10$  and  $N_e = 2-Z$

at magnetic fields  $\beta_Z \gtrsim 0.1$ . Up to date this is the most comprehensive investigation of ground state configurations for light to medium-heavy atoms and ions in strong magnetic fields. The data presented can be of special value for astrophysical applications, e.g., the modeling of neutron star atmospheres. A natural next step is the extension of this study to heavier elements up to iron, as they are assumed to exist in the atmospheres of neutron stars [38]. Also, the investigation of ground state configurations in the full range of magnetic fields from  $B = 0$  to the high-field ground state regime is an important task. We will pursue both directions in future work.

#### ACKNOWLEDGMENTS

This work was supported by Deutsche Forschungsgemeinschaft. We gratefully thank the bwGRiD project [39] for the computational resources.

- [1] M. V. Ivanov and P. Schmelcher, *Phys. Rev. A* **57**, 3793 (1998).  
 [2] M. V. Ivanov and P. Schmelcher, *Phys. Rev. A* **60**, 3558 (1999).  
 [3] M. V. Ivanov and P. Schmelcher, *Phys. Rev. A* **61**, 022505 (2000).  
 [4] M. D. Jones, G. Ortiz, and D. M. Ceperley, *Phys. Rev. A* **59**, 2875 (1999).  
 [5] A. Thirumalai and J. S. Heyl, *Phys. Rev. A* **79**, 012514 (2009).  
 [6] E. I. Tellgren, A. Soncini, and T. Helgaker, *J. Chem. Phys.* **129**, 154114 (2008).  
 [7] E. I. Tellgren, S. S. Reine, and T. Helgaker, *Phys. Chem. Chem. Phys.* **14**, 9492 (2012).

- [8] Z. Medin and D. Lai, *Phys. Rev. A* **74**, 062507 (2006).  
 [9] W. Becken, P. Schmelcher, and F. K. Diakonou, *J. Phys. B* **32**, 1557 (1999).  
 [10] W. Becken and P. Schmelcher, *J. Phys. B* **33**, 545 (2000).  
 [11] W. Becken and P. Schmelcher, *Phys. Rev. A* **63**, 053412 (2001).  
 [12] W. Becken and P. Schmelcher, *Phys. Rev. A* **65**, 033416 (2002).  
 [13] O. A. Al-Hujaj and P. Schmelcher, *Phys. Rev. A* **70**, 033411 (2004).  
 [14] O. A. Al-Hujaj and P. Schmelcher, *Phys. Rev. A* **70**, 023411 (2004).

- [15] K. K. Lange, E. I. Tellgren, M. R. Hoffmann, and T. Helgaker, *Science* **337**, 327 (2012).
- [16] C. Schimeczek, S. Boblest, D. Meyer, and G. Wunner, *Phys. Rev. A* **88**, 012509 (2013).
- [17] K. Mori and C. J. Hailey, *Astrophys. J.* **648**, 1139 (2006).
- [18] K. Mori and W. C. G. Ho, *Mon. Not. R. Astron. Soc.* **377**, 905 (2007).
- [19] A. K. Harding and D. Lai, *Rep. Prog. Phys.* **69**, 2631 (2006).
- [20] F. Özel, *Rep. Prog. Phys.* **76**, 016901 (2013).
- [21] H. Ruder, G. Wunner, H. Herold, and F. Geyer, *Atoms in Strong Magnetic Fields* (Springer, Heidelberg, 1994).
- [22] Y. P. Kravchenko, M. A. Liberman, and B. Johansson, *Phys. Rev. A* **54**, 287 (1996).
- [23] C. Schimeczek and G. Wunner, *Comput. Phys. Commun.* **185**, 614 (2014).
- [24] V. B. Pavlov-Verevkin and B. I. Zhilinskii, *Phys. Lett. A* **78**, 244 (1980).
- [25] K. A. U. Lindgren and J. T. Virtamo, *J. Phys. B* **12**, 3465 (1979).
- [26] Z. Chen and S. P. Goldman, *Phys. Rev. A* **45**, 1722 (1992).
- [27] P. Schmelcher and L. S. Cederbaum, *Phys. Rev. A* **43**, 287 (1991).
- [28] P. Schmelcher, *Phys. Rev. A* **52**, 130 (1995).
- [29] V. G. Bezchastnov, *J. Phys. B* **28**, 167 (1995).
- [30] D. Baye and M. Vincke, *J. Phys. B* **19**, 4051 (1986).
- [31] C. de Boor, *J. Approx. Theory* **6**, 50 (1972).
- [32] C. Schimeczek, D. Engel, and G. Wunner, *Comput. Phys. Commun.* **183**, 1502 (2012).
- [33] G. Ortiz, D. M. Ceperley, and R. M. Martin, *Phys. Rev. Lett.* **71**, 2777 (1993).
- [34] B. L. Hammond, W. A. Lester, Jr., and P. J. Reynolds, *Monte Carlo Methods in ab initio Quantum Chemistry*, World Scientific Lecture and Course Notes in Chemistry (World Scientific Publishing Co. Pte. Ltd., Singapur, 1994).
- [35] P. J. Knowles and N. C. Handy, *Chem. Phys. Lett.* **111**, 315 (1984).
- [36] J. von Neumann and E. P. Wigner, *Phys. Z.* **30**, 467 (1929).
- [37] J. Simola and J. Virtamo, *J. Phys. B* **11**, 3309 (1978).
- [38] M. Rajagopal, R. W. Romani, and M. C. Miller, *Astrophys. J.* **479**, 347 (1997).
- [39] bwGRiD, member of the German D-Grid initiative, funded by the Ministry of Education and Research (Bundesministerium für Bildung und Forschung) and the Ministry for Science, Research, and Arts Baden-Wuerttemberg (Ministerium für Wissenschaft, Forschung und Kunst Baden-Württemberg), <http://www.bw-grid.de>, Tech. Rep. (Universities of Baden-Württemberg, 2007-2013).